OXIDISED PHOSPHATIDYLCHOLINES INDUCE MULTIPLE FUNCTIONAL DEFECTS IN AIRWAY EPITHELIAL CELLS

Christopher D Pascoe[1,2], Neilloy Roy[1,2], Emily Turner-Brannen[1,2], Alexander Schultz[1,2], Amir Ravandi[1,3], Andrew J Halayko[1,2], Adrian R West[1,2]

1, Department of Physiology and Pathophysiology, University of Manitoba, MB, Canada
2, Biology of Breathing Group, Children's Hospital Research Institute of Manitoba, MB, Canada
3, Institute of Cardiovascular Sciences, St. Boniface Hospital Albrechtsen Research Centre, MB Canada

Correspondence
Dr Adrian R West
Children's Hospital Research Institute of Manitoba
606A John Buhler Research Centre
715 McDermot Avenue
Winnipeg MB R3E 3P4
Canada
Email: adrian.west@umanitoba.ca
Phone: +1 204 789 3603

Grants
1. Natural Sciences and Engineering Research Council, Discovery Grant (Adrian West)
2. Research Manitoba, New Investigator Operating Grant (Adrian West)
3. Research Manitoba, Postdoctoral Fellowship (Christopher Pascoe)
4. Canadian Respiratory Research Network Fellowship (Christopher Pascoe)
5. Canadian Institutes of Health Research, Banting Postdoctoral Fellowship (Christopher Pascoe)
6. Research Manitoba, Graduate Studentship (Neilloy Roy)
7. Canada Research Chairs Program (Andrew Halayko)
8. Canadian Institutes of Health Research Emerging Network: Canadian Respiratory Research Network (Andrew Halayko

The grant bodies had no role in study design, data collection and analysis, decision to publish, or preparation of the manuscript.

Short Title
Oxidised phosphatidylcholines impair epithelial barrier

Keywords
Airway epithelium
Epithelial barrier
Wound healing
Oxidative stress
Lipid peroxide
Asthma

ABSTRACT

Oxidative stress is a hallmark of numerous airway diseases, contributing to extensive cell and tissue damage. Cell membranes and the airway mucosal lining are rich in phospholipids that are particularly susceptible to oxidative attack, producing bioactive molecules including oxidized phosphatidylcholines (OxPC). With the recent discovery of elevated OxPC in animal models of asthma and asthmatic patients, we hypothesized that OxPC directly contribute to disease by inducing airway epithelial cell dysfunction.

We found that OxPC induced dose-dependent cell stress and loss of viability in a range of epithelial cell types. These responses corresponded with significant epithelial barrier dysfunction, which was further compounded when combining OxPC with an epithelial wound. OxPC significantly inhibited DNA synthesis and migration required for wound healing, but cells recovered if OxPC were washed off soon after treatment. OxPC induced extensive generation of reactive oxygen species that could not be abrogated by blockers of putative OxPC receptors, and caused extensive lipid peroxidation that could only be partially inhibited by the antioxidant n-acetyl cysteine. These outcomes were accompanied by profound mitochondrial dysfunction, raising the possibility that OxPC cause pathological lipid metabolism in a self-propagating cycle that contributes to disease pathogenesis.

In summary, we have identified OxPC as a group of bioactive molecules that significantly impairs multiple facets of epithelial cell function, consistent with pathological features of asthmatic epithelium. Further characterisation of the mechanisms by which OxPC affect epithelial cells could yield new insights into how oxidative stress contributes to the pathogenesis of airway disease.

INTRODUCTION

Asthma is a chronic disease of the airways which is characterized by inflammation, structural cell dysfunction, and excessive airway narrowing. Many of the features of asthma have been linked to reactive oxygen species (ROS) produced endogenously and upon exposure to environmental insults including air pollution, allergens, and smoke (46). ROS cause damage to tissues and cellular components and can act as a potent promoter of pro-inflammatory signals (43, 61, 62). Indeed, in airway epithelial cells, ROS enhances IL-8 production and reduces the activity of HDAC2 (27), which has been linked with steroid refractoriness in asthma (8, 33). In asthmatic patients, the abundance of ROS in the serum is correlated with the degree of airway hyperresponsiveness (AHR) and acute exacerbations of asthma requiring hospitalization (7, 14).

ROS are capable of damaging lipid membranes and the lipid-rich mucosal lining of the airways resulting in the production of a group of potent pro-inflammatory molecules collectively known as oxidized phosphatidylcholines, or OxPC (4). OxPC are produced from the poly-unsaturated fatty acid tails of phospholipids namely arachidonoyl and linoleoyl to form OxPAPC and OxPLPC respectively (17). In disease, OxPC promote the induction of atherogenic pathways in endothelial cells (19, 31), dose-dependently disrupt endothelial barrier function and induce adherens junction dissociation (3). OxPC are also associated with inflammatory pain, mediated by transient receptor potential channels TRPA1 and TRPV1 (36). In the lung, OxPC have been identified in mice and humans following infection with influenza and *Mycobacterium* (9, 32, 51) and in response to inhaled allergen challenge in asthma (28, 37). Some literature suggests that low doses of OxPC can act as inhibitors of toll-like receptor (TLR) signaling (11) however most research agrees that at physiological concentrations, they act as mediators of inflammation and disease (18, 40). In cultured airway smooth muscle cells, OxPC promote inflammation characterized by IL-6, IL-8, GM-CSF, and the production of pro-inflammatory lipid mediators (41, 42).

The airway epithelial cell plays an important role in protecting the underlying tissue from environmental irritants and coordinating inflammatory responses against microbes, and it is well established that dysfunction in the airway epithelium is an important factor asthma pathogenesis (25). With the recent identification of OxPC in the lungs of people with asthma and their well-established role in disrupting endothelial cell function in the vessels, we sought to establish their role in asthma pathogenesis through their ability to disrupt airway epithelial cell function. This manuscript is the first to show that OxPC promote airway epithelial cell dysfunction by disrupting their ability to form a protective barrier and impairing their self-repair capacity. Moreover, OxPC promote ongoing oxidative stress evidenced by the production of additional ROS and lipid peroxides, as well as profound mitochondrial dysfunction.

RESULTS

OxPC induce cell stress and loss of viability in airway epithelial cells

OxPC treatment resulted in dose-dependent LDH release, indicating cell stress in each cell type tested (Fig 1A). However, the magnitude of the effect was variable across epithelial cell lines with strong responses at low doses in BEAS-2B ($p<0.0001$, $n=5$), moderate responses in Calu-3 ($p<0.0001$, $n=5$), and weak responses in nHBE ($p<0.0001$, $n=5$) and ALI-nHBE ($p=0.0257$, $n=3$). High levels of cell stress were associated with loss of viability (Fig 1B); reduced cell viability was evident in BEAS-2B at OxPC doses as low as 10µg/mL ($p<0.0001$, $n=5$), and doses of 160 µg/mL were cytotoxic in Calu-3 ($p<0.0001$, $n=4$). No loss of viability was detected in nHBE ($p=0.2204$, $n=5$). Statistical significance was achieved in ALI-nHBE ($p=0.0438$, $n=3$), however the magnitude of

any effect was small relative to the other cell types, with no obvious dose-dependence and no significant differences relative to control in post-tests. The non-oxidizable negative control PSPC caused no quantitative or qualitative changes in this experiment, or in any subsequent experiment.

OxPC reversibly impair epithelial barrier function and wound healing

OxPC exposure at 80 and 160 µg/mL resulted in significant barrier impairment in Calu-3 cells, as measured by both paracellular permeability (Fig 2A; $p<0.0001$, $n=5$) and TEER assays (Fig 2B; interaction $p<0.0001$, time $p=0.0032$, OxPC $p<0.0001$, $n=4$). The 40 µg/mL dose trends towards barrier reinforcement by TEER but this effect was not significant. For ALI-nHBE, OxPC treatment did not cause any difference in permeability (Fig 2C; $p=0.5510$, $n=3$), and only a modest impairment of TEER (Fig 2D; interaction $p=0.9909$, time $p=0.0007$, OxPC $p=0.0232$, $n=3$). The effect on TEER appeared dose-dependent, but no significant differences were detectable.

Combining OxPC with a physical scratch revealed that the simultaneous 'two hits' could cause additional barrier dysfunction in Calu-3 cells (Fig 3A; interaction $p<0.0001$, time $p<0.0001$, OxPC $p<0.0001$, $n\geq4$). The 80 and 160 µg/mL groups displayed a profound failure of wound healing after 24 hours. Moreover, combining OxPC at 40 µg/mL with a scratch resulted in a significant delay in wound healing at 24-48 hours, in stark contrast to OxPC treatment alone. To further determine whether OxPC-induced-dysfunction is dependent on the overall degree of cell stress and is not necessarily permanent, scratched Calu-3 were exposed to 80 or 160 µg/mL OxPC for 24 or 72 hours, before the OxPC were washed off, and TEER re-measured after 24 hours. OxPC 80 µg/mL treated cells could partially recover barrier function (Fig 3B; $p=0.0079$, $n\geq4$) and the recovery was more complete with shorter exposure times. A single well of 160 µg/mL exposed cells saw a full recovery of TEER, but this maximal dose was otherwise terminal to barrier function.

In ALI-nHBE, OxPC at 160 µg/mL caused a modest but highly significant impairment of wound healing at 48 hours, with dose-dependent dysfunction persisting until 7 days (Fig 3C; interaction $p=0.8773$, time $p<0.0001$, OxPC $p<0.0001$).

OxPC reversibly inhibit DNA synthesis

Airway epithelial wound healing involves an initial migratory phase followed by increased proliferation at the wounded edge (59), thus we histologically assessed DNA synthesis to better understand wound healing dynamics (Fig 4). As expected, scratched cultures exhibit increased EdU labelling (indicative of DNA synthesis) compared with untreated controls, with qualitatively higher synthetic activity at the leading edge. In contrast, a submaximal 80 µg/mL OxPC dose results in a dramatic decrease in DNA synthesis at 24 hours ($p<0.0001$, $n=4$) and, qualitatively, the cells do not migrate to close the wound. DNA synthesis returns to control levels if OxPC

are left on the cells for 48 hours but experiences a dramatic rebound if OxPC are washed off the cells, without immediate wound closure. These results are entirely consistent with the barrier function results following both scratch and wash protocols.

OxPC do not regulate the mRNA abundance of epithelial phenotype markers

To determine whether barrier dysfunction was modulated by changes in the epithelial barrier phenotype, the relative mRNA abundance of three key phenotypic markers was measured after OxPC exposure (Fig 5). Neither e-cadherin (CDH1, p=0.4295, n=4) nor vimentin (VIM, p=0.4362, n=4) mRNA levels were altered by OxPC, suggesting maintenance of epithelial barrier phenotype and no acquisition of mesenchymal features. Zonula occludens 1 (TJP1) mRNA levels were significantly different across the groups in the ANOVA statistic (p=0.0069, n=4), however there was no linear dose-dependence and post-tests revealed no individual group differences. The small magnitude of the changes was below the realistic statistical limit of detection for RT-qPCR (54) suggesting that statistical differences in TJP1 levels have low biological relevance.

OxPC induce general ROS accumulation

The cell migration and proliferation processes required for wound healing require significant metabolic activity. To assess whether OxPC induce oxidative stress consistent with pathological respiration, we examined the effect of OxPC on ROS accumulation. OxPC rapidly induced general ROS accumulation in a time- and dose-dependent manner (Fig 6A-B; p<0.0001, n=7). To put these results in context of known disease-linked modulators, we performed separate experiments exposing cells to a maximal dose of house dust mite (HDM). General ROS accumulation was significantly elevated in response to HDM (p=0.0314, n=3), although the magnitude was markedly lower than a maximal OxPC dose.

To ascertain the specific cellular source of ROS, we assessed the accumulation of mitochondrial and cytosolic superoxide. Mitochondrial superoxide was not significantly altered by OxPC treatment (Fig 6C; p=0.3730, n=5), and no qualitative difference was apparent when compared with the brightly stained positive control (immunofluorescence microscopy; Fig 6D). Cytosolic superoxide reached statistical significance (Fig 6E; p=0.0227, n=5) however there was no obvious dose-dependence, post-tests were not significant, and the overall magnitude of any OxPC-related response was considerably lower than the corresponding positive control. Moreover, fluorescent imaging shows no qualitative difference between the control and maximal dose of OxPC relative to the much brighter positive control (Fig 6F). This indicates that cytoplasmic superoxide accumulation is unlikely to be biologically significant during OxPC exposure.

Receptor blockade does not mitigate OxPC-induced ROS accumulation

In other cell types, the negative effects of OxPC are associated with specific receptor-mediated pathways (30). To determine whether these pathways are responsible for our results in epithelial cells, Calu-3 were exposed to a maximal 160 µg/mL OxPC dose in the presence of putative OxPC receptor blockers (Fig 7). For each of the PAFR (WEB-2086; p=0.1179, n=3), EP2 (PF-04418948; p =0.5317, n=3), CD36 (SSO; p=0.7256, n=4) and TLR2/4 receptors (SsnB; p=0.1664, n=3), blocking agents did not inhibit general ROS accumulation. In contrast, the antioxidant NAC inhibited ROS in a dose-dependent manner, completely reversing ROS accumulation at 10 mM (p=0.0004, n=3).

OxPC induce additional lipid peroxidation

To determine whether ROS formation could induce ongoing cellular dysfunction, we assessed lipid peroxide generation. Similar to general ROS accumulation, lipid peroxides began accumulating rapidly after OxPC addition, with higher doses surpassing the level of lipid peroxides produced by the positive control cumene-OOH within 60 minutes (Fig 8A). At the 2-hour endpoint, all OxPC doses were significantly higher than control (Fig 8B; p<0.0001, n=4), with a very strong dose-dependency. In separate experiments, HDM was assessed for its ability to induce lipid peroxidation. The effect of HDM approached significance (p=0.0522, n=3), but the magnitude of the change was smaller than even the lowest dose of OxPC. Surprisingly, 10 mM NAC was only able to partially reverse the accumulation of lipid peroxides (Fig 8C; p=0.0001, n=7).

To validate these results and attempt to determine whether lipid peroxides were localised to any particular cellular compartment, lipid peroxidation was assessed by an alternative histological technique. OxPC induced a qualitative increase in lipid peroxides that were diffuse across the cell membrane and cytoplasm. There was no obvious segregation or punctate patterning that would indicate isolation to any specific organelle (Fig 8D).

Mitochondrial function is disrupted by OxPC treatment

Recent reports indicate that oxidised phospholipids accumulate in the mitochondria (58), and oxidised lipoproteins can cause mitochondrial membrane hyperpolarisation (20). Thus, we determined the effect of OxPC on Calu-3 mitochondrial membrane potential, as well as oxygen consumption during a mitochondrial stress test. Consistent with earlier work, OxPC induced a dose-dependent increase in TMRM staining, indicative of mitochondrial hyperpolarisation (Fig 9A; p<0.0001, n=6). Moreover, OxPC caused a profound alterations in oxygen consumption rate (OCR) during the stress test (Fig 9B; interaction p=0.0001, time p<0.0001, OxPC p<0.0001, n=4), with specific dose-dependent reductions in each of basal respiration (Fig 9C; p=0.0165), ATP-linked respiration (p<0.0001) and maximal respiration (p=0.0013), dose-dependent increases in proton leak (p=0.0002), but no change in non-mitochondrial respiration (p=0.0952).

DISCUSSION

Epithelial dysfunction and disease relevance

The airway epithelial barrier is the gateway to the lung and dysfunction of this barrier at a cellular level is associated with both asthma pathogenesis (26) and asthma severity (34). For this reason, we sought to explore the ability of OxPC to induce epithelial barrier dysfunction in the context of asthma. Our results indicate that OxPC can disrupt normal airway epithelial cell function and promoting pathologic features similar to those seen in the airways of people with asthma. This includes a loss of barrier integrity (22), impaired wound healing capacity (48), and further production of reactive oxygen species (12). This wide range of cellular dysfunction was accompanied by a profound disruption of mitochondrial metabolism, and each deleterious response was observed at doses below the threshold for detecting cell stress and loss of viability.

Wounding the epithelial layer increased the barrier-disrupting potency of OxPC, most notably in differentiated primary airway epithelial cells. This suggests that OxPC could be important in potentiating the negative effects of allergenic insults or other stressors in diseased airways. In this regard, exposing epithelial cells to HDM resulted in an increase in ROS that was considerably smaller than the level induced by low doses of OxPC. Additionally, OxPC exposure could stimulate further production of lipid peroxides indicating the potential for a self-propagating cycle that starts with allergen exposure. Interestingly, the negative effects of OxPC could be reversed following their removal suggesting that OxPC do not inherently cause permanent cell damage or irrecoverable activation of cell death pathways. Therefore, OxPC are potentially important molecules in the pathogenesis of asthma and interventions aimed at limiting their production or promoting their removal could be novel therapeutic options for this disease.

OxPC have been identified as a bioactive lipid molecule that have relevance to many chronic human diseases. In atherosclerosis, blocking the action of OxPC with the antibody E06 in mice reduced the amount of atherosclerosis and aortic valve calcifications (40). Following renal ischemia reperfusion injury in rats, there was a significant elevation in 55 OxPC species which correlated with the severity of the injury (47). Recently, members of our team have identified OxPC in the airways of mice and humans following allergen challenge and these were shown to be correlated with methacholine responsiveness following allergen challenge in people. In airway smooth muscle cells, OxPC promote an inflammatory phenotype, characterized by secretion of IL-6, IL-8, GM-CSF, the production of eicosanoids, and were controlled by signaling events through protein kinase C. Developing treatments that target the actions of OxPCs in the airways could offer us a better way to ameliorate the effects of oxidative stress in asthma, therefore augmenting our current treatment regimes.

Mechanisms of oxidative stress and lipid peroxidation

OxPC have been linked to signaling events involving PAFR, EP2, CD36 and TLR2/4 (30, 53). We were unable to show that any of these receptors were involved in mediating accumulation of ROS in response to OxPC in this study. Only pre-incubation with antioxidant NAC was able to reduce the cellular accumulation of ROS in response to OxPC. NAC operates as a cysteine source for the production of glutathione (45) and the glutathione anti-oxidant system is finely tuned for controlling cellular levels of lipid peroxides (56). In children with severe asthma, the oxidized glutathione levels are significantly elevated and reduced glutathione levels significantly repressed (16) indicating an elevated level of oxidative stress. Additionally, there exists single nucleotide polymorphisms (SNPs) in some of the genes for the glutathione-s-transferase enzymes that are associated with increased asthma risk (29, 49). Disequilibrium in the glutathione system could thus indicate a diminished ability to detoxify OxPC in the airways and make people with asthma particularly susceptible to the effects of OxPC. An alternative antioxidant mechanism for NAC involves triggering intracellular sulfane sulfur production which has antioxidant and cytoprotective functions (13). In this regard, treatments that increase endogenous production of sulfane sulfur could be useful in decreasing the antioxidant burden in asthma, specifically related to OxPC.

Despite the theoretical benefits of antioxidant treatments for asthma, results from animal and patient studies are mixed. With the exception of specific vitamin E isoforms that may specifically detoxify lipid peroxides (24, 39), dietary antioxidant supplementation seems to provide minimal benefit beyond a decrease in exhaled FeNO (1, 38, 50, 55). This may be consistent with our observations that NAC was unable to completely reverse lipid peroxidation, and that neither mitochondrial nor cytosolic superoxide are credible sources for the large magnitude of the dysfunction we observed. This raises the possibility that the primary pathology induced by OxPC is specifically associated with lipid metabolism. Xenobiotic metabolism involving cytochrome P450, lipoxygenase and cyclooxygenase are well known to produce lipid peroxide by-products and these reactions can be self-propagating in the presence of oxygen (2). However, our demonstration of profound mitochondrial dysfunction after OxPC exposure suggests direct interference with mitochondrial lipid metabolism enzymes (35) without necessarily producing a detectable superoxide intermediate. Metabolomic analysis of OxPC affected cells will be required to precisely determine which lipid peroxides are produced, the mitochondrial reactions/enzymes that are responsible, and how this process could be mitigated.

Differential cell responses

Intriguingly, we found significant differences in the responsiveness of different epithelial cells to OxPC exposure. This may represent a culturing artifact or altered metabolic requirements of undifferentiated epithelial cells and cell lines but may also highlight how OxPC may become disease relevant. Airway epithelium

from people with asthma exhibits an elevated number of basal cells and a reduction in the number of cells expressing E-cadherin (21) suggesting a more immature phenotype. In this regard, airway epithelium from asthma may be more susceptible to the effects of OxPC due to its relatively undifferentiated state, although it is important to note that the cells used in this study are not sourced from asthmatic patients. Alternatively, commercial supplements for culturing primary epithelial cells in ALI contain hydrocortisone which has been shown to inhibit the inflammatory response of cultured epithelial cells (15) and support mucociliary transport in cells (60). Importantly, glucocorticoids have been shown to increase the activity of antioxidant enzymes in asthma (10). We did not remove hydrocortisone from the media prior to experimentation which may have conferred some protection and only allowed us to observe negative effects on barrier function when OxPC was combined with a scratch. Finally, OxPC had a significant impact on DNA synthesis in our experiments suggesting that they may directly inhibit proliferation. Primary cells are relatively quiescent compared with the cell lines used in this study perhaps indicating that proliferating cells, or those that have an associated high metabolic requirement, are particularly susceptible to OxPC exposure. It will therefore be important to study how prolonged OxPC treatment alters the growth and differentiation trajectory of primary epithelial cells, to determine the effect on mucociliary phenotype and barrier function.

Summary

We have demonstrated that OxPC induce profound dose-dependent cellular dysfunction that may potentiate other stressors to manifest as impaired epithelial barrier function in diseased airways. Future work will need to ascertain whether the cellular dysfunction we have observed is a product of the combination and total quantity of OxPC applied, or can be attributable a single OxPC species operating through a specific mechanism. Understanding the role of individual OxPC in causing epithelial cell dysfunction will help us to identify potential treatment options that protect the cell or 'mop-up' OxPC in a more specific manner than NAC, more completely prevent lipid peroxide accumulation, and recover mitochondrial function. Finally, by using mice that express the anti-OxPC antibody (E06), and determining whether OxPC can augment the pathology associated with HDM exposure, it will be possible to ascertain whether OxPC are sufficient and necessary for the pathogenesis of airway disease.

ACKNOWLEDGEMENTS

Adrian West is supported by NSERC Discovery Grant # RGPIN-2014-06412 and a Research Manitoba New Investigator Operating Grant. Chris Pascoe is supported by a Research Manitoba Postdoctoral Fellowship, a Canadian Respiratory Research Network Fellowship and the Canadian Institutes of Health Research Banting Postdoctoral Fellowship. Neilloy Roy is supported by a Research Manitoba Graduate Studentship. Andrew

Halayko is supported by the Canada Research Chairs Program, and portions of this work were supported by funding from the CIHR Canadian Respiratory Research Network. The authors would like to thank Gerald Stelmack for assistance with Beas-2B cell culture.

AUTHOR CONTRIBUTIONS

Chris Pascoe co-wrote the manuscript, designed experiments, generated OxPC, and performed cell culture, ROS/superoxide assays, lipid peroxidation assays, and mitochondrial function assays.

Neilloy Roy performed paracellular permeability assays.

Emily Turner-Brannen performed cell culture, cell stress/viability assays, TEER measurements, mRNA abundance analysis, proliferation assays, and mitochondrial function assays.

Alexander Schultz performed HDM ROS and HDM lipid peroxide assays.

Amir Ravandi conceived methods to generate OxPC, and performed mass spectrometric assessment of the OxPC mixture.

Andrew Halayko helped conceive the study and in vitro protocols for using OxPC, edited the manuscript, generated OxPC, and supplied OxPC receptor inhibitors.

Adrian West conceived the study, co-wrote the manuscript, designed/supervised all aspects of experimentation, and performed data/statistical analysis, cell culture and TEER measurements.

METHODS

Cell Culture

Calu-3 human airway epithelial cells were purchased from ATTC (HTB-55). Cells were propagated in DMEM/F-12 (Gibco 11330057) supplemented with 10% heat inactivated fetal bovine serum (FBS) (Gibco 12483020) and 1% penicillin/streptomycin (Gibco 15140122). For all experiments, Calu-3 were trypsinized and re-seeded at a density of 2×10^5 cells/cm^2 onto Transwell membranes [12 mm diameter, 0.4 µm pore size (Corning 3460)], 18 mm round glass coverslips (VWR CA48382-041), 12-well plates (Sarstedt 83.3921), or Seahorse XF24 microplates (Agilent 100777-004) each coated with 3 µg/mL rat tail collagen I (Corning 354236) in PBS. Cells were maintained in growth media for 4 days before being serum-deprived for 48 hours in DMEM/F12 containing 0.5% FBS and 1% insulin-transferrin-selenium (ITS) supplement (Gibco 41400045).

Normal human bronchial epithelial cells were purchased from Lonza (CC-2540S, lot # 493462) and grown in PneumaCult™-Ex Plus Medium (Stemcell Technologies 05040). Cells at passage 2-3 were trypsinized and re-seeded onto 12-well plates (nHBE) or Transwells (ALI-nHBE) at a density of 1×10^5 cells/cm^2 and maintained in PneumaCult™-Ex Plus for 3-4 days. ALI-nHBE cells were then transferred to fully supplemented PneumaCult™-ALI Medium, exposed to an air-liquid interface, and maintained for ≥3 weeks for mucociliary differentiation, confirmed by the presence of mucus, ciliary activity, and establishment of epithelial barrier function (>500 Ω.cm^2).

BEAS-2B-GRE cells [gift from Dr. Rob Newton, previously described previously in (6)] were propagated in DMEM/F-12 supplemented with 10% FBS and 100 µg/mL G418, and seeded at a density of 3×10^3 cells/cm^2 in 12-well plates. Cells were grown until approximately 80% confluent then serum deprived for 24 hours in DMEM/F12 with 1% ITS.

Generation and Administration of Oxidised Lipids

OxPC were generated by exposing PAPC (1-palmitoyl-2-arachidonoyl-sn-glycero-3-phosphocholine, Avanti Polar Lipids 850459C) to room air for 4 days, during which PAPC visibly changed from a white to yellow paste. The non-oxidizable negative control PSPC (1-palmitoyl-2-stearoyl-sn-glycero-3-phosphocholine, Avanti Polar Lipids 850456C) was exposed to the same conditions and did not exhibit any visible changes. Treated OxPC/PSPC were resuspended in chloroform:methanol (2:1) at 1mg/mL and stored at -20°C under nitrogen gas to prevent further oxidation. The oxidation state of both lipid preparations has previously been confirmed by LC/MS/MS (58).

OxPC and PSPC were prepared for dosing by aliquoting an appropriate volume of lipid solution and evaporating the chloroform:methanol under a stream of sterile nitrogen. The remaining lipid was immediately resuspended in warm media or buffer as appropriate and added to the cells (Calu-3 on Transwells: 1 mL apical chamber, 0.5 mL basolateral chamber; Calu-3, nHBE and BEAS-2B-GRE in 12-well plates: 1 mL; ALI-nHBE on Transwells, 1 mL basolateral chamber, 75 µL apical chamber). For exposure times exceeding 3 days, cells were re-dosed with OxPC/PSPC in fresh media every 3-4 days.

Cell Stress and Viability

Cell stress was assessed by LDH release using the Roche Cytotoxicity Detection Kit (Roche 11644793001) in cells treated with OxPC (0-160 µg/mL) or PSPC (160 µg/mL) for 24 hours. Culture media was collected, gently centrifuged (150 × RCF for 4 minutes) and combined with the kit reagent for 10 min before absorbance readings were taken at 490 nm. LDH release was expressed as the percentage of LDH activity in the media relative to untreated control cells lysed with 2% triton X-100.

Cell viability was determined by the uptake and retention of neutral red dye. After 24-hour exposure to OxPC or PSPC, a 0.33% stock solution of neutral red in PBS was added 1:20 to the culture media and incubated for 2 hours. Cells were then gently rinsed with PBS and lysed in four times the original culture media volume with a solution of 1% acetic acid and 50% ethanol in H_2O. Net absorbance was then calculated as A_{540} minus A_{690}.

Epithelial Barrier Function

The effect of OxPC on epithelial barrier function in Calu-3 and ALI-nHBE under static and scratched conditions was determined by measuring paracellular permeability and transepithelial electrical resistance (TEER). Paracellular permeability (P, cm/s) was calculated using the steady state approximation equation for Transwells (5):

$$P = \frac{\Delta C_B}{\Delta t}\left(\frac{V_B}{A \cdot C_A}\right)$$

In brief, Transwells (surface area A = 1.13cm^2) were treated with OxPC or PSPC for 24 hours, washed with PBS, and the apical chamber loaded with 0.5 mL of 300 µg/mL (C_A) of sterile sodium fluorescein (NaFlu) (Sigma F6377) in Hank's Balanced Salt Solution (HBSS) (Gibco 14065056). Assessment was initiated by transferring Transwells to fresh 12-well plates containing 1.5 mL (V_B) per well HBSS, and monitoring NaFlu accumulation in the basolateral chamber at 37°C for 3 hours in a FLUOstar Optima fluorescence plate reader in orbital average mode (7 locations, 22 mm diameter, Ex: 460 nm Em: 520 nm). Fluorescence time curves for each Transwell were converted to basolateral concentration (C_B, µg/mL) time curves using a fluorescence-concentration

standard curve. The slope of the linear segment of these concentration-time curves ($\Delta C_B/\Delta t$, µg/mL/s) was then determined using the linear regression function of GraphPad Prism 6.07.

TEER was measured with a freshly calibrated MilliCell ERS-02 Voltohmmeter (Millipore). Baseline TEER was measured in PBS prior to cell seeding and subtracted from all experimental measurements, and net TEER was normalised to an equivalent untreated and non-scratched control to account for temporal variability. For wound healing experiments, cells were scratched with a sterile 10 µL pipet tip and firm pressure, washed once with PBS, and post-wound TEER readings taken. Cells were then treated with media containing OxPC or PSPC as appropriate, and TEER monitored for up to 14 days.

DNA synthesis as a metric of proliferation

DNA synthesis was assessed by thymidine-analog incorporation and histological detection using the Click-iT EdU Imaging Kit (Thermo Fisher C10337). Confluent serum-deprived Calu-3 cells were scratched, washed, and incubated with OxPC (80 µg/mL) for up to 48 hours before being pulsed with 10 µM 5-ethynyl-2'-deoxyuridine (EdU) for 2 hours. The cells were then fixed with 4% paraformaldehyde (PFA) in PBS for 15 minutes, washed twice with 3% BSA in PBS and permeabilized with 0.5% triton X-100 in PBS for 20 minutes. EdU fluorescent labelling was performed per the manufacturers instruction's, before nuclei were counterstained with 0.2 µg/mL Hoechst 33342 (Thermo Fisher H1399) in PBS for 10 minutes. Coverslips were mounted with SlowFade Diamond (Thermo Fisher S36967) before being sealed with nail varnish and imaged on an Olympus IX-51 fluorescent microscope. Images of at least 3 fields from each coverslip (minimum 1000 cells per 'n') were captured at consistent exposure settings, before EdU positive and total nuclei were manually counted with ImageJ.

mRNA abundance

The mRNA abundance for epithelial phenotype markers was assessed by RT-qPCR. Calu-3 were treated with OxPC or PSPC for 18 hours before total RNA was isolated by the Ambion Purelink RNA Mini Kit (Thermo Fisher 12183025) before RNA concentration and purity were assessed by A_{260}:A_{280} spectrophotometry. Reverse transcription was performed with 1 µg total RNA using iScript Reverse Transcription Supermix for RT-qPCR (Biorad 170-8841). cDNA equivalent to 20 ng of total RNA was then amplified in duplicate using SsoAdvanced Universal SYBR Green Supermix (Biorad 172-5274) and 300 nM of the appropriate primers (Table 1) in a Biorad CFX96 thermal cycler. Cycling conditions involved 30 s incubation at 95°C for polymerase activation, followed by 40 cycles of denaturing at 95°C for 10 s and annealing/extension at 58°C for 30 s. Crossing thresholds (Ct) were calculated and housekeeping gene stability confirmed (M value <0.25) using the Biorad CFX Manager 3.1 software, and mean reaction efficiency (E) was determined using LinRegPCR 2017.0 (44). Relative mRNA

abundance was calculated using efficiency-corrected ΔCt ($E^{\Delta Ct}$) divided by a normalizing factor (NF) derived from the geometric mean of $E^{\Delta Ct}$ for two stable housekeeping genes (23, 52). The final data was scaled such that untreated control condition presented a mean result of 1 AU.

Oxidative Stress

The capacity of OxPC and house dust mite extract (HDM, Greer XPB82D3A2.5) to induce the accumulation of general cytosolic ROS, cytosolic superoxide and mitochondrial superoxide in Calu-3 were assessed by dichlorofluorescein (DCF), dihydroethidium (DHE) and MitoSOX assays respectively. For DCF assays, serum-deprived Calu-3 were loaded with 10µM DCF (Sigma D6883) in low-serum media for 30 minutes, then washed with warm Hanks Balanced Salt Solution (HBSS). Cells were then incubated with OxPC, PSPC, HDM (100 µg/mL) or positive control cumene hydroperoxide (cumene-OOH, 200 µM) in HBSS, and fluorescence quantified in a FLUOstar Optima (Ex 492, Em 520) for 2 hours. In separate experiments, cells were pre-incubated for 2 hours with vehicle control (0.1% DMSO), inhibitors of ROS [N-acetyl-L-cysteine (NAC), Sigma-Aldrich A7250], or blockers of receptors associated with OxPC activity including platelet activating factor receptor (WEB-2086, Tocris 2339), prostaglandin EP2 receptor (PF-04418948, Tocris 4814), CD36 [sulfosuccinimidyl oleate (SSO), Cayman Chemical 11211] and toll like receptors 2 and 4 [sparstolonin B (SsnB), Sigma-Aldrich SML1767]. Cells were then loaded with DCF and co-incubated with inhibitors, OxPC (160 µg/mL) and vehicle control (0.1% DMSO) for a further 2 hours before measuring fluorescence.

For DHE and MitoSOX assays, cells were pre-incubated with OxPC, PSPC, or positive controls doxorubicin (50 µM; New England Biolabs 5927) and antimycin A (10 µM; Sigma-Aldrich A8674) for 2 hours in low-serum media. Cells were then stained with 5µM DHE (Thermo Fisher D1168) for 30 minutes or 5µM MitoSOX (Thermo Fisher M36008) for 15 minutes and counterstained with H33342 for 10 minutes. Fluorescence intensity was quantified in a FLUOstar Optima (DHE and MitoSOX: Ex 485, Em 590), and cells were imaged by fluorescence microscopy. Exposure was set using the appropriate positive control condition, all images taken at consistent settings.

Lipid Peroxidation Assays

The generation of lipid peroxides in response to OxPC- and HDM-induced-ROS was quantitatively assessed in Calu-3 with the Image-iT Lipid Peroxidation Kit (Thermo Fisher C10445). Calu-3 cells were loaded with 10 µM BODIPY-C11 in HBSS for 30 minutes, washed three times with PBS, and treated with OxPC, PSPC, HDM (100 µg/mL) or cumene-OOH in HBSS for 2 hr. The progress of lipid peroxidation was monitored as the ratio of oxidised to reduced BODIPY-C11 at 37°C for 2 hours in a Cytation 5MPV (fluorescence intensity 5×5 area scanning, Oxidised Ex: 478/20 nm Em 520/20 nm, Reduced Ex: 566/20 nm Em 606/20 nm).

The sub-cellular location of lipid peroxides was determined with the Click-iT Lipid Peroxidation Imaging Kit (Thermo Fisher C10446). Calu-3 cells were simultaneously loaded with 50 µM linoleamide alkyne (LAA) and treated with OxPC in HBSS for 2 hours. Cells were then washed with PBS, fixed in 4% PFA for 15 minutes then permeabilized in 4% PFA with 0.5% triton X-100. After 3 washes in PBS cells were blocked with 1% BSA for 30 minutes and LAA fluorescent labelling was performed per the manufacturer's instructions. Cells were then counterstained, mounted and imaged as described above.

Mitochondrial Function

Mitochondrial membrane potential was assessed in live cells using the fluorescent dye tetramethylrhodamine (TMRM; Biotium 70017). Briefly, Calu-3 were treated with OxPC or PSPC for 2-hours and then stained with 0.1 µM TMRM in HBSS for 30-minutes. The oxidative phosphorylation uncoupler CCCP (2 µM, Sigma C2759) was used as a negative control to establish baseline/minimal mitochondrial membrane potential. Excess TMRM dye was removed with HBSS and the degree of fluorescence intensity relative to the CCCP condition was measured in a FLUOstar Optima (Ex 548, Em 573 nm).

Oxygen consumption rate (OCR) was measured during Seahorse XF Cell Mito Stress Tests as per the user guide (Agilent 103015-100) with modifications. In brief, Calu-3 in Seahorse plates were switched to Seahorse XF base media (Agilent 103334-100) supplemented with 10 mM glucose (Fisher BP350), 1 mM sodium pyruvate (Gibco 11360070) and 2 mM Glutamax (Gibco 35050061) and treated with OxPC such that the first baseline OCR reading was timed 2 hr after exposure. Seahorse Sensor Cartridges (Agilent 100867-100) were hydrated for 6-18 hours at 37 °C in 1 mL of the supplied calibrant. Stock solutions of stress test reagents were prepared by dissolving in DMSO, diluting to 10× desired final concentrations with supplemented media, before adding to the appropriate sensor ports. The sensor cartridge was calibrated in a Seahorse XF24 Analyzer, cell plates installed, and OCR measured for 30 min at baseline, and in response to 2 µM oligomycin (New England Biolabs 9996L), 0.5 µM FCCP (Simga C2920), and 0.5 µM rotenone/antimycin-A (Sigma R8875 and A8674 respectively). Triplicate technical replicates on each plate were averaged to produce final OCR datapoints, and parameters of mitochondrial function calculated according to the user guide.

Data Analysis and Statistics

All numerical data are presented as mean ± standard error. Each 'n' value represents a fully independent experiment created from a separate flask of stock cells. Statistical tests were performed with the GraphPad Prism 6.07 software package, with $p<0.05$ considered statistically significant. Matched samples 1-way ANOVA was used for all OxPC experiments where data was collected at a single time-point, with Dunnett post-tests

calculated against control or OxPC 160 µg/mL conditions as appropriate. In TEER recovery experiments, all pairwise Bonferroni post-tests were calculated. For time-course experiments, independent samples 2-way ANOVA (factors: OxPC, time) was performed, with Dunnett post-tests calculated against the control or PSPC 160 µg/mL conditions as appropriate. Paired t-test was used for all HDM experiments.

TABLE 1.

Primers used for mRNA abundance analysis by RT-qPCR. Primers were selected using Primer-BLAST [http://www.ncbi.nlm.nih.gov/tools/primer-blast/ (57)] to span exon-exon junctions to prevent amplification of genomic DNA, with primer specificity continually assessed by melting curve analysis.

Common name (code), function	Forward primer (5' – 3')	Reverse Primer	Accession no. (amplicon location)	Efficiency (stability; M)
Glyceraldehyde-3-phosphate dehydrogenase (GAPDH), housekeeping	CTGACTTCAACAGCGACACC	CGTTGTCATACCAGGAAATGAG	NM_002046.5 (1039-1137)	1.955 (0.216)
14-3-3 protein zeta/delta (YWHAZ), housekeeping	TCCCCAGAGAAAGCCTGCTC	ATCCGATGTCCACAATGTCAAG	NM_003406.3 (688-831)	1.962 (0.216)
e-cadherin (CDH1), barrier marker	GCTGGACCGAGAGAGTTTCC	GCTGTTGTGCTTAACCCCTC	NM_004360.3 (1120-1200)	2.039
Zonula occludens-1 (TJP1), barrier marker	GAAATCGCACAGTTTGGCAC	GCTGAAGGACTCACAGGAATAG	NM_003257.4 (5200-5334)	2.003
Vimentin (VIM), mesenchymal marker	ATCCAAGTTTGCTGACCTCTC	TCAGTGGACTCCTGCTTTGC	NM_003380.3 (1289-1366)	1.942

FIGURES

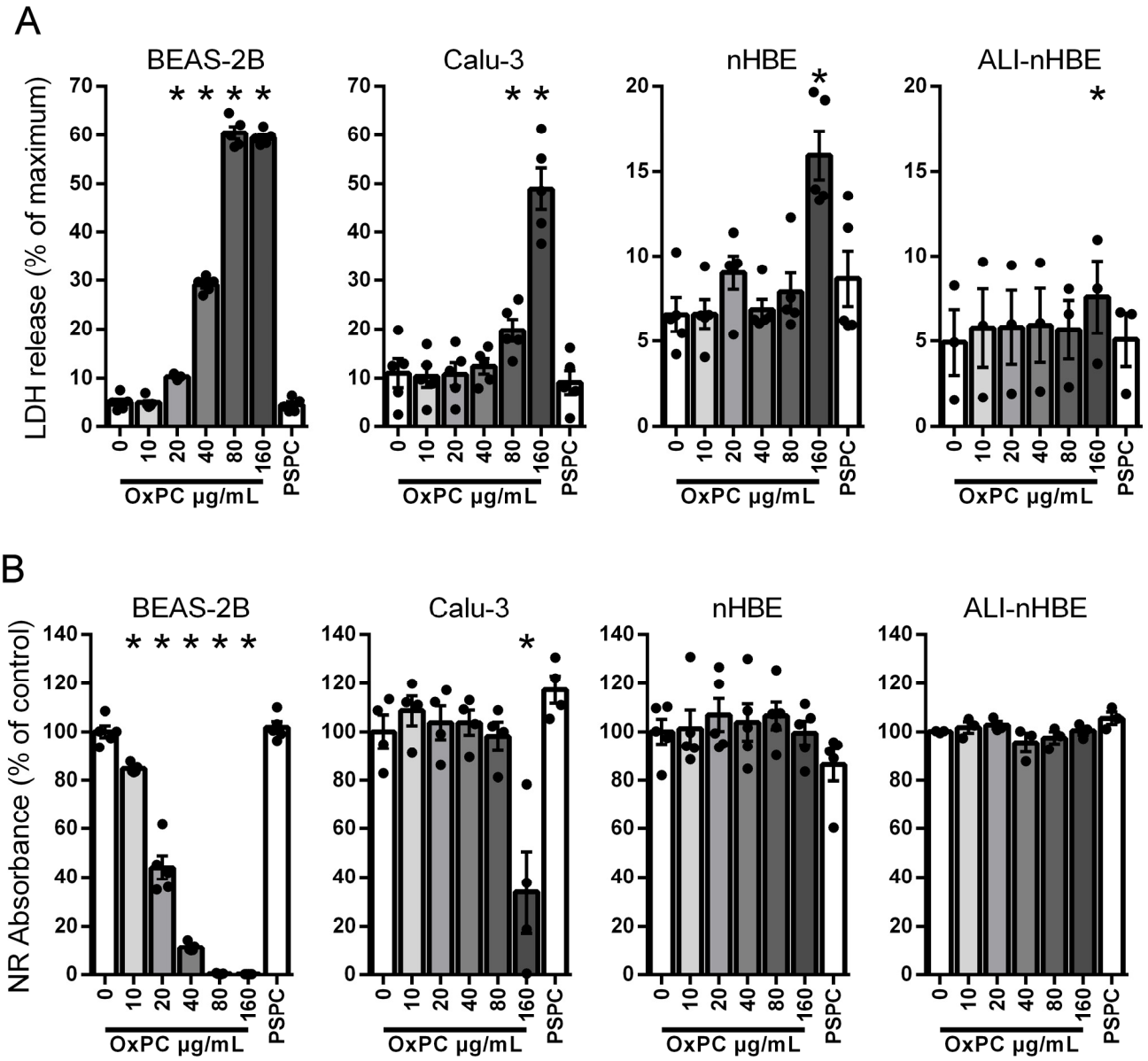

Figure 1.

OxPC induces cell stress (A; increased LDH release) and loss of cell viability (B; reduced NR absorbance) in a dose-dependent and cell-specific manner. BEAS-2B were particularly sensitive experiencing almost complete cell death at 40 µg/mL OxPC (stress $p<0.0001$, viability $p<0.0001$, $n=5$). Calu-3 were moderately sensitive (stress $p<0.0001$, viability $p<0.0001$, $n\geq4$), with nHBE (stress $p<0.0001$, viability $p=0.2204$, $n=5$) and ALI-nHBE (stress $p=0.0257$, viability $p=0.0438$, $n=3$) being relatively robust. * represents a significant difference from the 0 µg/mL OxPC control condition.

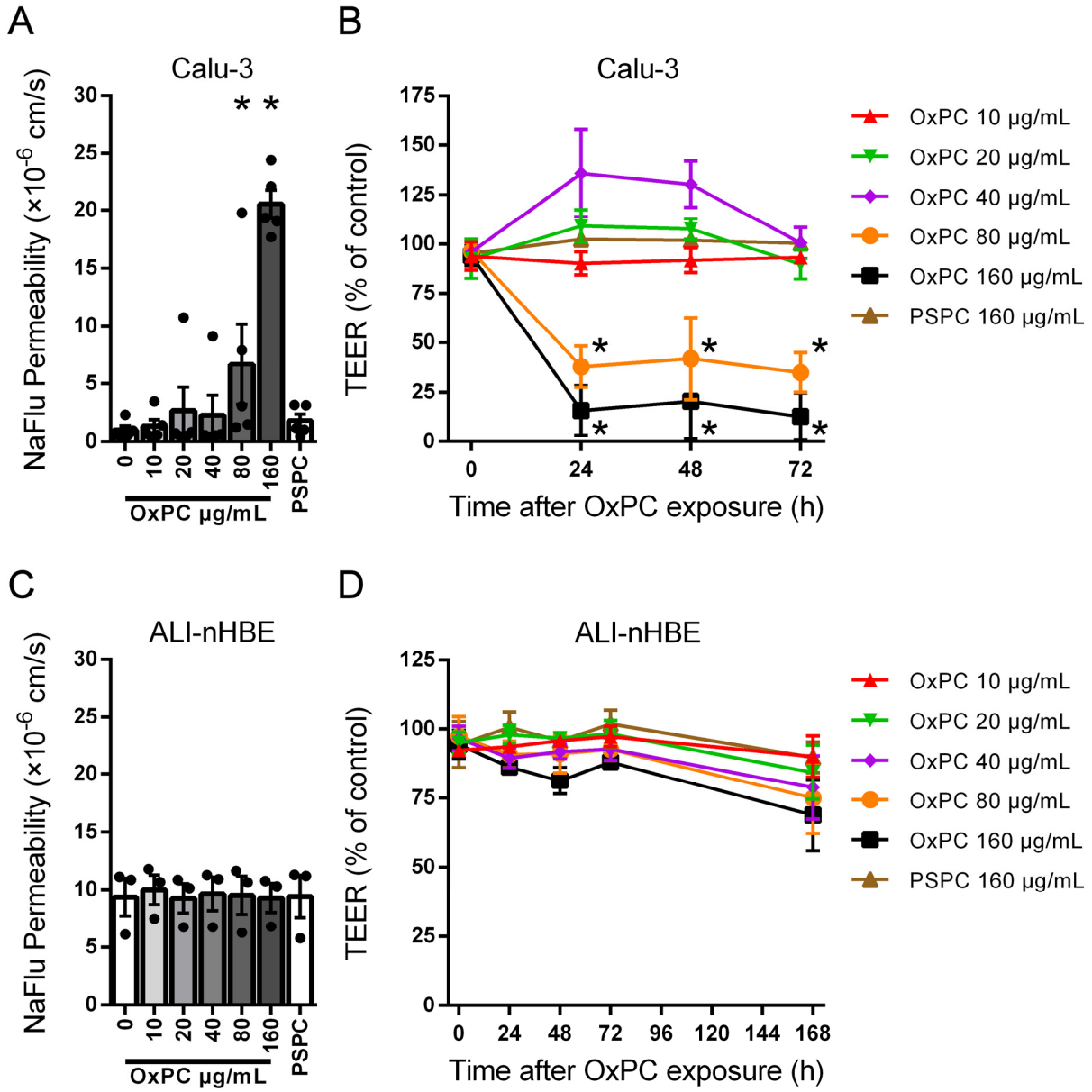

Figure 2.

Under static conditions, barrier function was impaired by OxPC in a dose-dependent and cell-specific manner. Calu-3 exhibited functional defects in both paracellular permeability (A; $p<0.0001$, n=5) and TEER (B; interaction $p<0.0001$, time $p=0.0032$, OxPC $p<0.0001$, n=4) at 80-160 µg/mL. The effect of OxPC on ALI-nHBE is not significant for permeability (C; $p=0.5510$, n=3) and only modestly significant for TEER (D; interaction $p=0.9909$, time $p=0.0007$, OxPC $p=0.0232$, n=3), but post-tests do not indicate significance for any group or timepoint. * represents difference from the 0 µg/mL OxPC control condition (permeability) or PSPC (TEER) conditions.

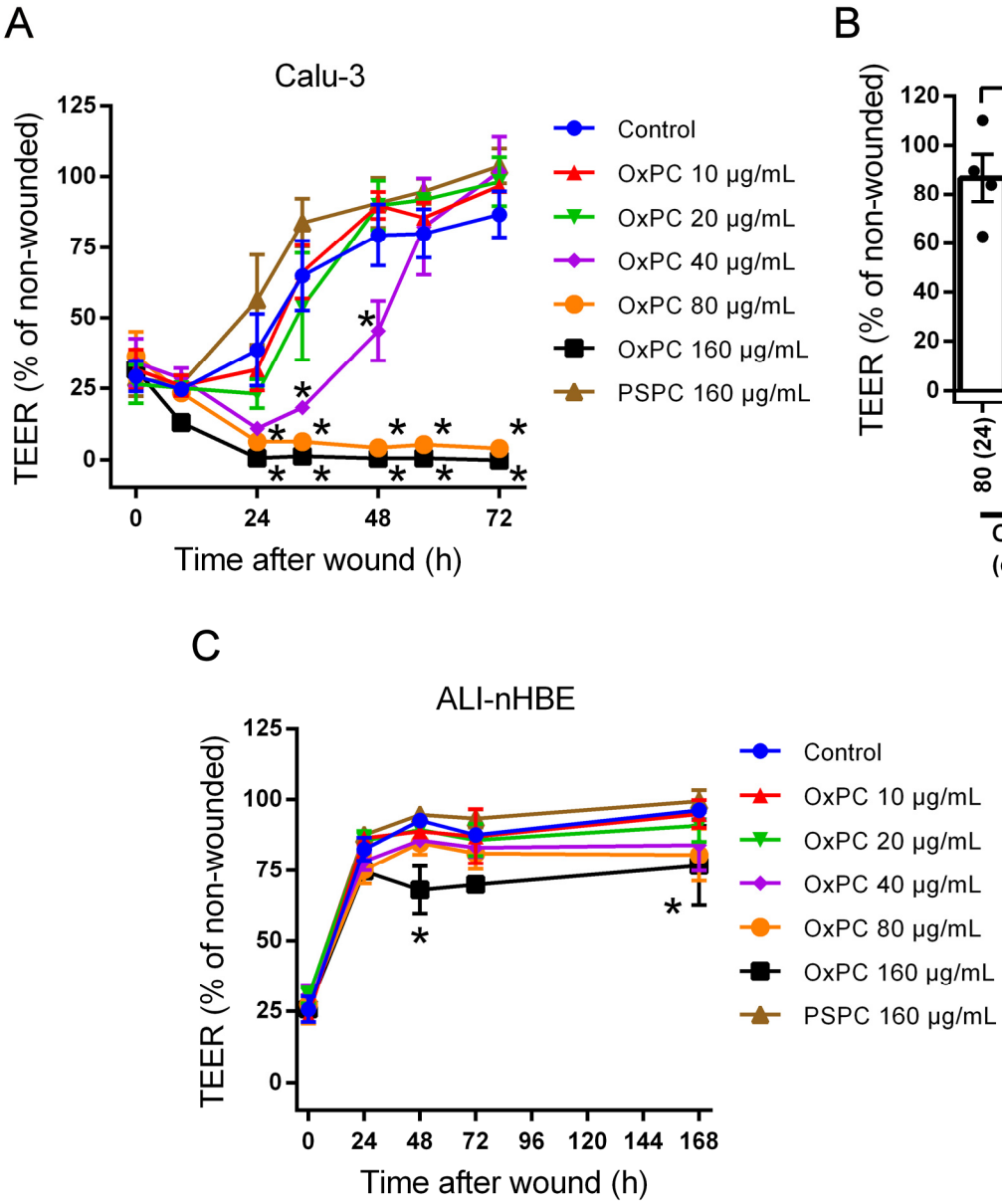

Figure 3.

OxPC treatment potentiates barrier dysfunction after a scratch. In Calu-3 cells, OxPC at 40 µg/mL significantly delayed wound healing (contrast with the lack of defect at 40 µg/mL in Fig 2B) with profound dysfunction at 80-160 µg/mL (A; interaction $p<0.0001$, time $p<0.0001$, OxPC $p<0.0001$, $n\geq4$). However, barrier function could partially recover in the 80 µg/mL condition if OxPC are rapidly washed off (B; $p=0.0079 n\geq4$). Scratched ALI-nHBE cultures display defective wound healing in the OxPC 160 µg/mL group (C; interaction $p=0.8773$, time $p<0.0001$, OxPC $p<0.0001$) that is not evident in static cultures (contrast with the lack of defect at 160 µg/mL in Fig 2D). * represents significant difference from the 0 µg/mL OxPC control condition (wound healing) or between conditions (washout recovery).

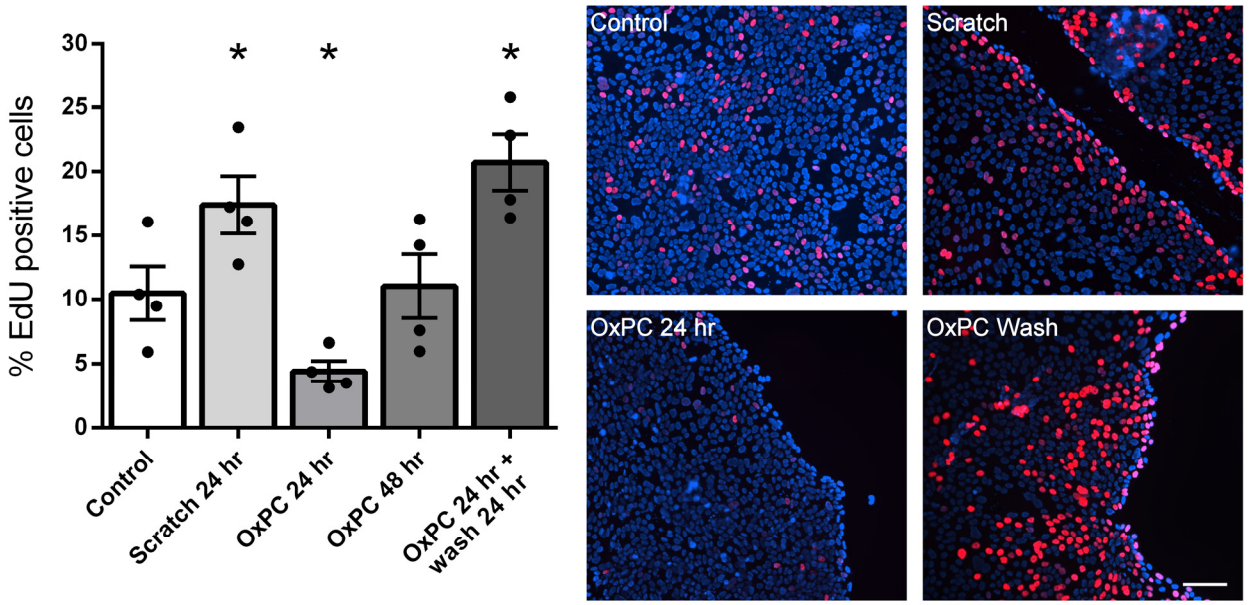

Figure 4.

DNA synthesis in Calu-3 cells is upregulated on the leading edge after a scratch, but this is significantly inhibited by 80 µg/mL OxPC ($p<0.0001$, n=4). DNA synthesis recovers if OxPC are washed off, but without immediate wound closure. * represents significant difference from the 0 µg/mL OxPC control condition. Scale bar is 100 µm.

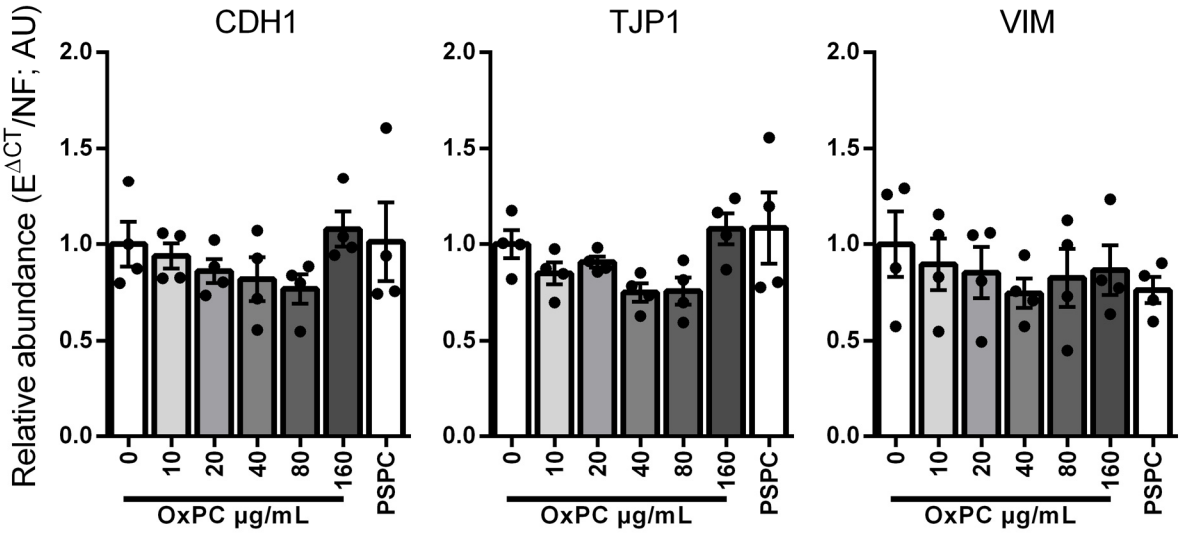

Figure 5.

Markers for epithelial and barrier phenotype are not appreciably regulated by OxPC in Calu-3 cells. The mRNA abundance of CDH1 (p=0.4295, n=4) and VIM (p=0.4362, n=4) were not significantly altered after OxPC treatment. While statistical significance was detected for TJP1 mRNA levels (p=0.0069, n=4), the small magnitude of the changes and lack of dose-dependency makes it unlikely that modulation of this gene is responsible for the observed barrier dysfunction.

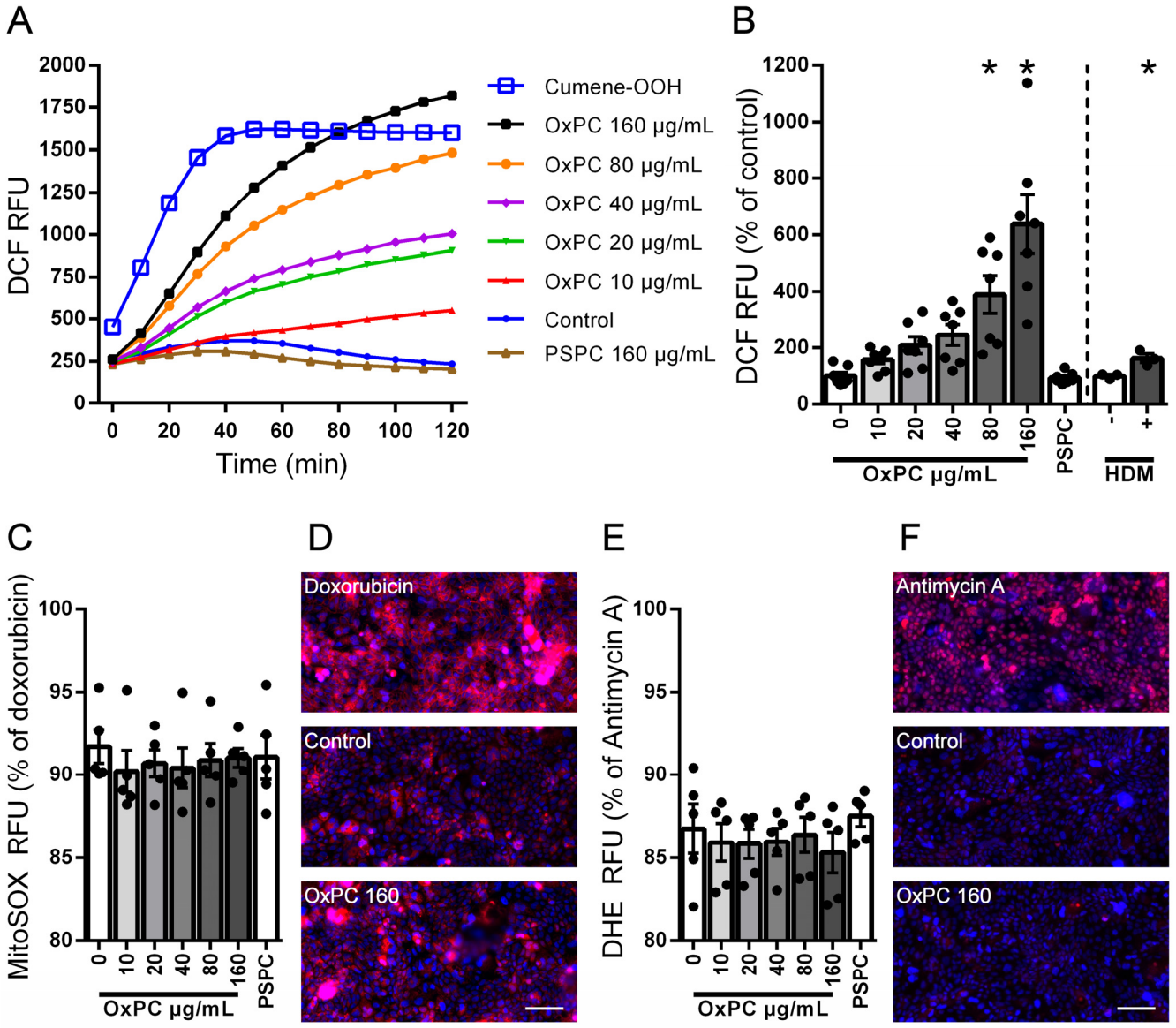

Figure 6.

OxPC induce time- (A) and dose-dependent (B) general ROS accumulation in Calu-3 cells ($p<0.0001$, n=7). HDM is also capable of inducing ROS accumulation ($p=0.0314$, n=3), but with a much smaller magnitude. Mitochondrial (C-D; $p=0.3730$, n=5) and cytosolic (E-F; $p=0.0227$, n=5) superoxide are only marginally influenced by OxPC, with no obvious dose-dependence and significantly lower signal than their respective positive controls. * represents significant difference from the 0 µg/mL OxPC control condition. Scale bar is 100 µm.

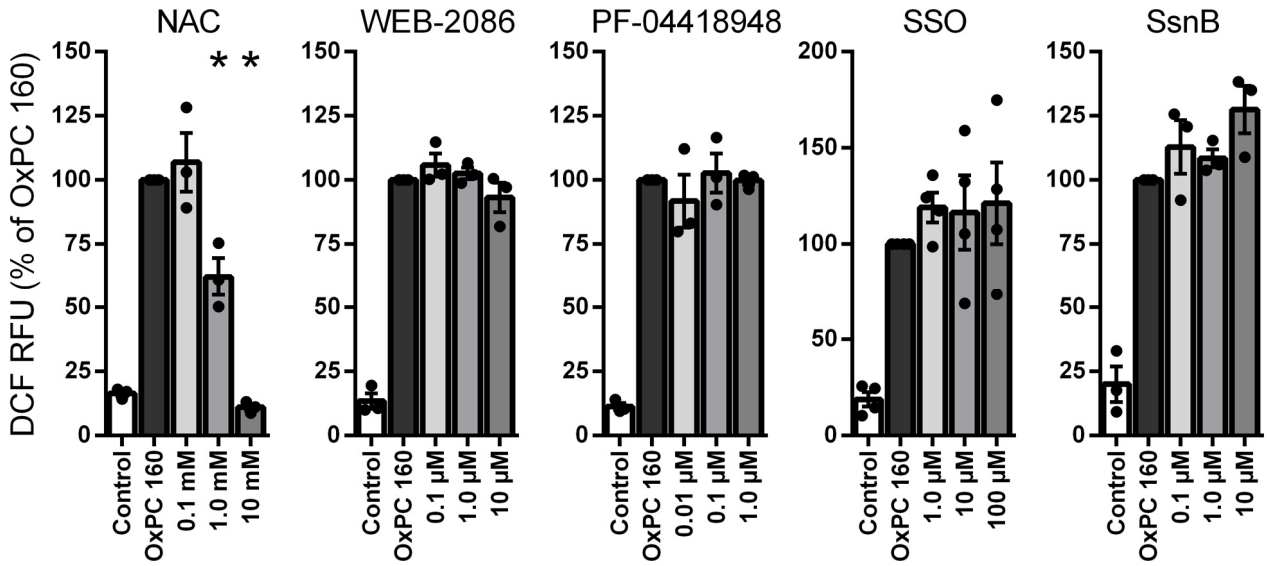

Figure 7.

General ROS accumulation induced by OxPC could be abrogated by the antioxidant NAC (p=0.0004, n=3). However, inhibitors of established OxPC receptors PAFR (WEB-2086; p=0.1179, n=3), EP2 (PF-04418948; p =0.5317, n=3), CD36 (SSO; p=0.7256, n=4) and TLR2/4 (SsnB; p=0.1664, n=3) each had no effect. * represents significant difference (i.e., inhibition) from the OxPC 160 µg/mL condition. Untreated Controls are shown for reference in each graph but are not included in the statistics.

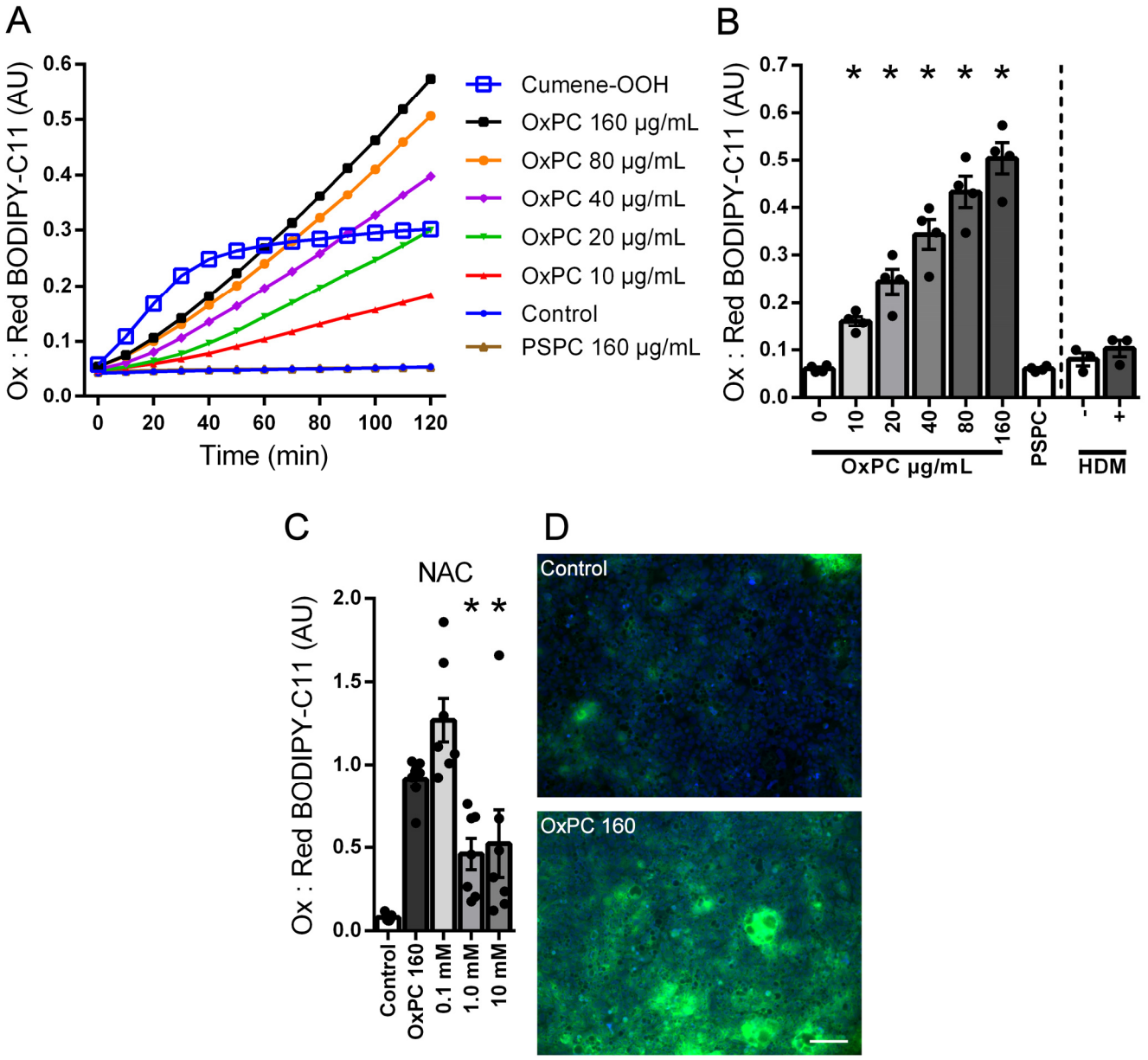

Figure 8.

OxPC induce time- (A) and dose-dependent (B) generation of lipid peroxides in Calu-3 cells ($p<0.0001$, n=4). The effect of HDM was modest in comparison and not statistically significant ($p=0.0522$, n=3). In contrast to general ROS, 10 mM NAC could only partially reverse lipid peroxidation (C; $p=0.0001$, n=7). Assessing lipid peroxidation by an alternative histological technique (D) confirms significant accumulation that did not appear to be localised to any specific cell membrane or organelle. * represents significant difference from the 0 µg/mL OxPC control condition (B) and from the OxPC 160 µg/mL condition (C). Scale bar is 100 µm.

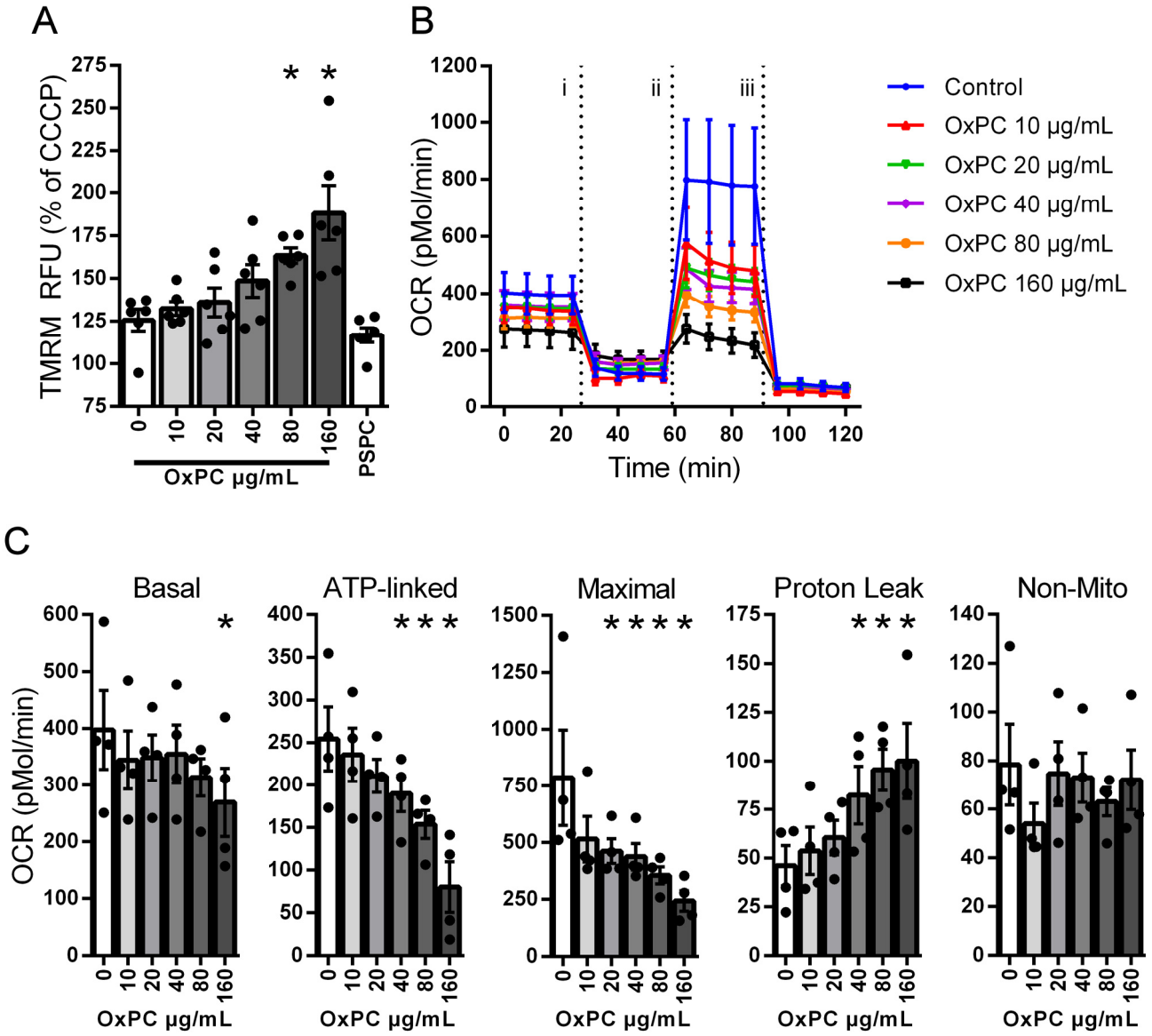

Figure 9.

OxPC induce dose-dependent increase in TMRM fluorescence, indicative of mitochondrial membrane hyperpolarisation (A; $p<0.0001$, n=6). Reductions in OCR (interaction $p=0.0001$, time $p<0.0001$, OxPC $p<0.0001$, n=4) are apparent during mitochondrial stress tests (B; i=oligomycin, ii=FCCP, iii=rotenone/antimycin-A), and calculation of distinct metabolic parameters (C) reveals dose-dependent reductions in basal ($p=0.0165$), ATP-linked ($p<0.0001$) and maximal respiration ($p=0.0013$), dose-dependent increases in proton leak ($p=0.0002$), but no change in non-mitochondrial respiration ($p=0.0952$). These combined responses are indicative of profound mitochondrial dysfunction in response to OxPC challenge. * represents significant difference from the 0 µg/mL OxPC control condition.

REFERENCES

1. **Aliyali M, Poorhasan Amiri A, Sharifpoor A, and Zalli F**. Effects of N-acetylcysteine on asthma exacerbation. *Iran J Allergy Asthma Immunol* 9: 103-109, 2010.
2. **Ayala A, Munoz MF, and Arguelles S**. Lipid peroxidation: production, metabolism, and signaling mechanisms of malondialdehyde and 4-hydroxy-2-nonenal. *Oxid Med Cell Longev* 2014: 360438, 2014.
3. **Birukova AA, Starosta V, Tian X, Higginbotham K, Koroniak L, Berliner JA, and Birukov KG**. Fragmented oxidation products define barrier disruptive endothelial cell response to OxPAPC. *Transl Res* 161: 495-504, 2013.
4. **Bochkov VN, Oskolkova OV, Birukov KG, Levonen AL, Binder CJ, and Stockl J**. Generation and biological activities of oxidized phospholipids. *Antioxid Redox Signal* 12: 1009-1059, 2010.
5. **Buchert M, Turksen K, and Hollande F**. Methods to examine tight junction physiology in cancer stem cells: TEER, paracellular permeability, and dilution potential measurements. *Stem Cell Rev* 8: 1030-1034, 2012.
6. **Chivers JE, Cambridge LM, Catley MC, Mak JC, Donnelly LE, Barnes PJ, and Newton R**. Differential effects of RU486 reveal distinct mechanisms for glucocorticoid repression of prostaglandin E release. *Eur J Biochem* 271: 4042-4052, 2004.
7. **Comhair SA, Ricci KS, Arroliga M, Lara AR, Dweik RA, Song W, Hazen SL, Bleecker ER, Busse WW, Chung KF, Gaston B, Hastie A, Hew M, Jarjour N, Moore W, Peters S, Teague WG, Wenzel SE, and Erzurum SC**. Correlation of systemic superoxide dismutase deficiency to airflow obstruction in asthma. *Am J Respir Crit Care Med* 172: 306-313, 2005.
8. **Cosio BG, Mann B, Ito K, Jazrawi E, Barnes PJ, Chung KF, and Adcock IM**. Histone acetylase and deacetylase activity in alveolar macrophages and blood mononocytes in asthma. *Am J Respir Crit Care Med* 170: 141-147, 2004.
9. **Cruz D, Watson AD, Miller CS, Montoya D, Ochoa MT, Sieling PA, Gutierrez MA, Navab M, Reddy ST, Witztum JL, Fogelman AM, Rea TH, Eisenberg D, Berliner J, and Modlin RL**. Host-derived oxidized phospholipids and HDL regulate innate immunity in human leprosy. *J Clin Invest* 118: 2917-2928, 2008.
10. **De Raeve HR, Thunnissen FB, Kaneko FT, Guo FH, Lewis M, Kavuru MS, Secic M, Thomassen MJ, and Erzurum SC**. Decreased Cu,Zn-SOD activity in asthmatic airway epithelium: correction by inhaled corticosteroid in vivo. *Am J Physiol* 272: L148-154, 1997.
11. **Erridge C, Kennedy S, Spickett CM, and Webb DJ**. Oxidized phospholipid inhibition of toll-like receptor (TLR) signaling is restricted to TLR2 and TLR4: roles for CD14, LPS-binding protein, and MD2 as targets for specificity of inhibition. *J Biol Chem* 283: 24748-24759, 2008.
12. **Erzurum SC**. New Insights in Oxidant Biology in Asthma. *Ann Am Thorac Soc* 13 Suppl 1: S35-39, 2016.
13. **Ezerina D, Takano Y, Hanaoka K, Urano Y, and Dick TP**. N-Acetyl Cysteine Functions as a Fast-Acting Antioxidant by Triggering Intracellular H2S and Sulfane Sulfur Production. *Cell Chem Biol* 25: 447-459 e444, 2018.
14. **Fatani SH**. Biomarkers of oxidative stress in acute and chronic bronchial asthma. *J Asthma* 51: 578-584, 2014.
15. **Feinstein MB, and Schleimer RP**. Regulation of the action of hydrocortisone in airway epithelial cells by 11beta-hydroxysteroid dehydrogenase. *Am J Respir Cell Mol Biol* 21: 403-408, 1999.
16. **Fitzpatrick AM, Teague WG, Holguin F, Yeh M, Brown LA, and Severe Asthma Research P**. Airway glutathione homeostasis is altered in children with severe asthma: evidence for oxidant stress. *J Allergy Clin Immunol* 123: 146-152 e148, 2009.
17. **Fruhwirth GO, Loidl A, and Hermetter A**. Oxidized phospholipids: from molecular properties to disease. *Biochim Biophys Acta* 1772: 718-736, 2007.
18. **Furnkranz A, Schober A, Bochkov VN, Bashtrykov P, Kronke G, Kadl A, Binder BR, Weber C, and Leitinger N**. Oxidized phospholipids trigger atherogenic inflammation in murine arteries. *Arterioscler Thromb Vasc Biol* 25: 633-638, 2005.
19. **Gargalovic PS, Imura M, Zhang B, Gharavi NM, Clark MJ, Pagnon J, Yang WP, He A, Truong A, Patel S, Nelson SF, Horvath S, Berliner JA, Kirchgessner TG, and Lusis AJ**. Identification of inflammatory gene modules

based on variations of human endothelial cell responses to oxidized lipids. *Proc Natl Acad Sci U S A* 103: 12741-12746, 2006.

20. **Giovannini C, Matarrese P, Scazzocchio B, Sanchez M, Masella R, and Malorni W**. Mitochondria hyperpolarization is an early event in oxidized low-density lipoprotein-induced apoptosis in Caco-2 intestinal cells. *FEBS Lett* 523: 200-206, 2002.

21. **Hackett TL, Singhera GK, Shaheen F, Hayden P, Jackson GR, Hegele RG, Van Eeden S, Bai TR, Dorscheid DR, and Knight DA**. Intrinsic phenotypic differences of asthmatic epithelium and its inflammatory responses to respiratory syncytial virus and air pollution. *Am J Respir Cell Mol Biol* 45: 1090-1100, 2011.

22. **Heijink IH, Nawijn MC, and Hackett TL**. Airway epithelial barrier function regulates the pathogenesis of allergic asthma. *Clin Exp Allergy* 44: 620-630, 2014.

23. **Hellemans J, Mortier G, De Paepe A, Speleman F, and Vandesompele J**. qBase relative quantification framework and software for management and automated analysis of real-time quantitative PCR data. *Genome Biol* 8: R19, 2007.

24. **Hernandez ML, Wagner JG, Kala A, Mills K, Wells HB, Alexis NE, Lay JC, Jiang Q, Zhang H, Zhou H, and Peden DB**. Vitamin E, gamma-tocopherol, reduces airway neutrophil recruitment after inhaled endotoxin challenge in rats and in healthy volunteers. *Free Radic Biol Med* 60: 56-62, 2013.

25. **Holgate ST**. Epithelium dysfunction in asthma. *J Allergy Clin Immunol* 120: 1233-1244; quiz 1245-1236, 2007.

26. **Holgate ST, Davies DE, Puddicombe S, Richter A, Lackie P, Lordan J, and Howarth P**. Mechanisms of airway epithelial damage: epithelial-mesenchymal interactions in the pathogenesis of asthma. *Eur Respir J Suppl* 44: 24s-29s, 2003.

27. **Ito K, Hanazawa T, Tomita K, Barnes PJ, and Adcock IM**. Oxidative stress reduces histone deacetylase 2 activity and enhances IL-8 gene expression: role of tyrosine nitration. *Biochem Biophys Res Commun* 315: 240-245, 2004.

28. **Jha A, Pascoe CD, Ravandi A, Halayko AJ, and Carlsten C**. Oxidized Phosphatidylcholine in Human Airways Upon Exposure to Allergen and/or Diesel Exhaust. In: *C103. OUTDOOR AIR POLLUTION: EPIDEMIOLOGY AND MECHANISMS*p. A6834-A6834.

29. **Kamada F, Mashimo Y, Inoue H, Shao C, Hirota T, Doi S, Kameda M, Fujiwara H, Fujita K, Enomoto T, Sasaki S, Endo H, Takayanagi R, Nakazawa C, Morikawa T, Morikawa M, Miyabayashi S, Chiba Y, Tamura G, Shirakawa T, Matsubara Y, Hata A, Tamari M, and Suzuki Y**. The GSTP1 gene is a susceptibility gene for childhood asthma and the GSTM1 gene is a modifier of the GSTP1 gene. *Int Arch Allergy Immunol* 144: 275-286, 2007.

30. **Lee S, Birukov KG, Romanoski CE, Springstead JR, Lusis AJ, and Berliner JA**. Role of phospholipid oxidation products in atherosclerosis. *Circ Res* 111: 778-799, 2012.

31. **Lee S, Li R, Kim B, Palvolgyi R, Ho T, Yang QZ, Xu J, Szeto WL, Honda H, and Berliner JA**. Ox-PAPC activation of PMET system increases expression of heme oxygenase-1 in human aortic endothelial cell. *J Lipid Res* 50: 265-274, 2009.

32. **Lee YH, Lai CL, Hsieh SH, Shieh CC, Huang LM, and Wu-Hsieh BA**. Influenza A virus induction of oxidative stress and MMP-9 is associated with severe lung pathology in a mouse model. *Virus Res* 178: 411-422, 2013.

33. **Li LB, Leung DY, Martin RJ, and Goleva E**. Inhibition of histone deacetylase 2 expression by elevated glucocorticoid receptor beta in steroid-resistant asthma. *Am J Respir Crit Care Med* 182: 877-883, 2010.

34. **Masuyama K, Morishima Y, Ishii Y, Nomura A, Sakamoto T, Kimura T, Mochizuki M, Uchida Y, and Sekizawa K**. Sputum E-cadherin and asthma severity. *J Allergy Clin Immunol* 112: 208-209, 2003.

35. **Mayr JA**. Lipid metabolism in mitochondrial membranes. *J Inherit Metab Dis* 38: 137-144, 2015.

36. **Oehler B, Kistner K, Martin C, Schiller J, Mayer R, Mohammadi M, Sauer RS, Filipovic MR, Nieto FR, Kloka J, Pflucke D, Hill K, Schaefer M, Malcangio M, Reeh PW, Brack A, Blum R, and Rittner HL**. Inflammatory pain control by blocking oxidized phospholipid-mediated TRP channel activation. *Sci Rep* 7: 5447, 2017.

37. **Pascoe CD, Edel AL, El-Gammal A, Ravandi A, Gauvreau GM, O'Byrne P, and Halayko AJ**. Peroxidation of Phosphatidylcholine: A Signature for Allergen-Induced Airway Responses and Allergen Specificity. In: *D98.*

*INSIGHTS INTO ENVIRONMENTAL EXPOSURES IN ASTHMA, COPD, AND CONSTRICTIVE BRONCHIOLITIS*p. A7338-A7338.

38. **Patel BD, Welch AA, Bingham SA, Luben RN, Day NE, Khaw KT, Lomas DA, and Wareham NJ**. Dietary antioxidants and asthma in adults. *Thorax* 61: 388-393, 2006.

39. **Peh HY, Ho WE, Cheng C, Chan TK, Seow AC, Lim AY, Fong CW, Seng KY, Ong CN, and Wong WS**. Vitamin E Isoform gamma-Tocotrienol Downregulates House Dust Mite-Induced Asthma. *J Immunol* 195: 437-444, 2015.

40. **Que X, Hung MY, Yeang C, Gonen A, Prohaska TA, Sun X, Diehl C, Maatta A, Gaddis DE, Bowden K, Pattison J, MacDonald JG, Yla-Herttuala S, Mellon PL, Hedrick CC, Ley K, Miller YI, Glass CK, Peterson KL, Binder CJ, Tsimikas S, and Witztum JL**. Oxidized phospholipids are proinflammatory and proatherogenic in hypercholesterolaemic mice. *Nature* 558: 301-306, 2018.

41. **Ragheb M, Stelmack G, Jha A, and Halayko AJ**. Oxidized Phosphatidylcholine Induces COX2 Gene Expression and Cytokine Secretion by Human Airway Smooth Muscle Cells. In: *C108. GETTING INFLAMED: MARKERS OF LUNG INJURY AND REMODELLING*p. A6944-A6944.

42. **Ragheb M, Stelmack G, Jha A, Kindrachuk J, and Halayko AJ**. Unraveling the Signaling Pathways Involved with the Pro-Inflammatory Features of Oxidized Phoshphatidylcholine in Airway Smooth Muscle. In: *D58. AIRWAYS HYPERRESPONSIVENESS: NOVEL MECHANISMS AND TARGETS*p. A7262-A7262.

43. **Riedl MA, and Nel AE**. Importance of oxidative stress in the pathogenesis and treatment of asthma. *Curr Opin Allergy Clin Immunol* 8: 49-56, 2008.

44. **Ruijter JM, Ramakers C, Hoogaars WM, Karlen Y, Bakker O, van den Hoff MJ, and Moorman AF**. Amplification efficiency: linking baseline and bias in the analysis of quantitative PCR data. *Nucleic Acids Res* 37: e45, 2009.

45. **Rushworth GF, and Megson IL**. Existing and potential therapeutic uses for N-acetylcysteine: the need for conversion to intracellular glutathione for antioxidant benefits. *Pharmacol Ther* 141: 150-159, 2014.

46. **Sahiner UM, Birben E, Erzurum S, Sackesen C, and Kalayci O**. Oxidative stress in asthma. *World Allergy Organ J* 4: 151-158, 2011.

47. **Solati Z, Edel AL, Shang Y, O K, and Ravandi A**. Oxidized phosphatidylcholines are produced in renal ischemia reperfusion injury. *PLoS One* 13: e0195172, 2018.

48. **Stevens PT, Kicic A, Sutanto EN, Knight DA, and Stick SM**. Dysregulated repair in asthmatic paediatric airway epithelial cells: the role of plasminogen activator inhibitor-1. *Clin Exp Allergy* 38: 1901-1910, 2008.

49. **Tamer L, Calikoglu M, Ates NA, Yildirim H, Ercan B, Saritas E, Unlu A, and Atik U**. Glutathione-S-transferase gene polymorphisms (GSTT1, GSTM1, GSTP1) as increased risk factors for asthma. *Respirology* 9: 493-498, 2004.

50. **Tenero L, Piazza M, Zanoni L, Bodini A, Peroni D, and Piacentini GL**. Antioxidant supplementation and exhaled nitric oxide in children with asthma. *Allergy Asthma Proc* 37: e8-13, 2016.

51. **Van Lenten BJ, Wagner AC, Navab M, Anantharamaiah GM, Hui EK, Nayak DP, and Fogelman AM**. D-4F, an apolipoprotein A-I mimetic peptide, inhibits the inflammatory response induced by influenza A infection of human type II pneumocytes. *Circulation* 110: 3252-3258, 2004.

52. **Vandesompele J, De Preter K, Pattyn F, Poppe B, Van Roy N, De Paepe A, and Speleman F**. Accurate normalization of real-time quantitative RT-PCR data by geometric averaging of multiple internal control genes. *Genome Biol* 3: RESEARCH0034, 2002.

53. **Walton KA, Hsieh X, Gharavi N, Wang S, Wang G, Yeh M, Cole AL, and Berliner JA**. Receptors involved in the oxidized 1-palmitoyl-2-arachidonoyl-sn-glycero-3-phosphorylcholine-mediated synthesis of interleukin-8. A role for Toll-like receptor 4 and a glycosylphosphatidylinositol-anchored protein. *J Biol Chem* 278: 29661-29666, 2003.

54. **Weaver S, Dube S, Mir A, Qin J, Sun G, Ramakrishnan R, Jones RC, and Livak KJ**. Taking qPCR to a higher level: Analysis of CNV reveals the power of high throughput qPCR to enhance quantitative resolution. *Methods* 50: 271-276, 2010.

55. **Wood LG, Garg ML, Smart JM, Scott HA, Barker D, and Gibson PG**. Manipulating antioxidant intake in asthma: a randomized controlled trial. *Am J Clin Nutr* 96: 534-543, 2012.

56. **Yang Y, Cheng JZ, Singhal SS, Saini M, Pandya U, Awasthi S, and Awasthi YC**. Role of glutathione S-transferases in protection against lipid peroxidation. Overexpression of hGSTA2-2 in K562 cells protects against hydrogen peroxide-induced apoptosis and inhibits JNK and caspase 3 activation. *J Biol Chem* 276: 19220-19230, 2001.
57. **Ye J, Coulouris G, Zaretskaya I, Cutcutache I, Rozen S, and Madden TL**. Primer-BLAST: a tool to design target-specific primers for polymerase chain reaction. *BMC Bioinformatics* 13: 134, 2012.
58. **Yeang C, Hasanally D, Que X, Hung MY, Stamenkovic A, Chan D, Chaudhary R, Margulets V, Edel AL, Hoshijima M, Gu Y, Bradford W, Dalton N, Miu P, Cheung DY, Jassal DS, Pierce GN, Peterson KL, Kirshenbaum LA, Witztum JL, Tsimikas S, and Ravandi A**. Reduction of myocardial ischaemia-reperfusion injury by inactivating oxidized phospholipids. *Cardiovasc Res* 115: 179-189, 2019.
59. **Zahm JM, Kaplan H, Herard AL, Doriot F, Pierrot D, Somelette P, and Puchelle E**. Cell migration and proliferation during the in vitro wound repair of the respiratory epithelium. *Cell Motil Cytoskeleton* 37: 33-43, 1997.
60. **Zaidman NA, Panoskaltsis-Mortari A, and O'Grady SM**. Differentiation of human bronchial epithelial cells: role of hydrocortisone in development of ion transport pathways involved in mucociliary clearance. *Am J Physiol Cell Physiol* 311: C225-236, 2016.
61. **Zuo L, He F, Sergakis GG, Koozehchian MS, Stimpfl JN, Rong Y, Diaz PT, and Best TM**. Interrelated role of cigarette smoking, oxidative stress, and immune response in COPD and corresponding treatments. *Am J Physiol Lung Cell Mol Physiol* 307: L205-218, 2014.
62. **Zuo L, Otenbaker NP, Rose BA, and Salisbury KS**. Molecular mechanisms of reactive oxygen species-related pulmonary inflammation and asthma. *Mol Immunol* 56: 57-63, 2013.